Fracture evaluation of plasticized polylactic acid / poly (3-HYDROXYBUTYRATE) blends for commodities replacement in packaging applications

M.L. Iglesias Montes [a], V.P. Cyras [a,b], L.B. Manfredi [a,b], V. Pettarín [a,c], L.A. Fasce [a,b,*]

[a] Instituto de Investigaciones en Ciencia y Tecnología de Materiales (INTEMA), Facultad de Ingeniería, Universidad Nacional de Mar del Plata - Consejo Nacional de Investigaciones Científicas y Técnicas (CONICET), Av. Colón 10850, 7600, Mar del Plata, Argentina
[b] Departamento de Ingeniería Química y en Alimentos, Facultad de Ingeniería, Universidad Nacional de Mar del Plata, J. B. Justo 4302, 7600, Mar del Plata, Argentina
[c] Departamento de Ingeniería en Materiales, Facultad de Ingeniería, Universidad Nacional de Mar del Plata, J. B. Justo 4302, 7600, Mar del Plata, Argentina

ABSTRACT

Nowadays, scientific and technological efforts are being carried out to diminish serious ecological problems caused by indiscriminate use of non-biocompostable polymers in the packaging industry. In this sense, novel biodegradable blends of different composition based on poly(lactic acid) (PLA), poly(3-hydroxybutyrate) (PHB) and tributyrin (TB) are developed and here proposed as an eco-friendly alternative. Materials are characterized by fracture experiments under quasi-static and biaxial impact loading. Fracture behavior is analyzed together with thermal, tensile and water permeation properties to evaluate their potential in-service performance. TB_PLA/PHB blends with 15 wt% TB exhibit better permeation and fracture toughness than currently used bio-based polymers, being in the range of polyethylene properties. Results highlight the potential of these new blends broadening the current application field of PLA.

1. Introduction

The packaging industry is one of the markets with the highest consumption of plastics worldwide, generating serious ecological problems due to the indiscriminate use of synthetic packaging films that do not biodegrade and accumulate in the atmosphere [1]. Consequently, scientific researches oriented to the study of biodegradable and bio-based polymers and their blends and composites, have gained special interest in the packaging industry. Their extreme versatility and ability to be processed into sheets and thin films make them the perfect replacement of commodities by eco-friendly packaging materials. Biodegradable aliphatic polyesters, such as poly(lactic acid) (PLA), poly-hydroxyalkanoates (PHA) and polycaprolactone (PCL) are the subject of intensive and applied researches. Among them, poly(lactic acid) (PLA), which is obtained from renewable resources and is the most competitive biodegradable polymer in the market [2], and poly(3-hydroxybutyrate) (PHB), which is produced by microorganisms, are very promising bio-polymers with potential for the intended applications.

Both PLA and PHB are semi-crystalline polymers that exhibit high strength and stiffness but low fracture toughness and brittle behavior at

room temperature, which limit their applications. Brittleness is attributed to the high glass transition temperature of PLA [3] and to the high crystalline degree and relatively large spherulites of PHB [4]. In addition, PLA has better mechanical performance than PHB while PHB displays better barrier properties [5–7]. Several authors have proposed blending PLA and PHB as a strategy to modify unfavorable characteristics and improve properties of each pristine polymer [8–12]. In general, PLA/PHB mixtures exhibit better barrier properties than PLA [6, 13], but still relatively low strain at break values (improvements lower than 1%) [8,11]. To overcome this drawback, the incorporation of plasticizers have been proposed, resulting in a decrease in glass transition temperature (Tg), a better material processability and an improvement in its flexibility [6,8,14,15]. For example, elongation at break values (ε_b) reported for PLA/PHB (75:25 w/w) blended with different plasticizers are in the range of 6%–15% for poly(ethylene glycol) (PEG) [6], D-limonene [11] and Lapol 108 [8], and 90% for acetyltributylcitrate (ATBC) [14]. In addition, acetyl tributyl citrate (ATBC) have also proved to be effective in accelerating the disintegration process under composting conditions [14].

An attractive alternative plasticizer is tributyrin (TB). TB is a

---

hydrophobic triglyceride present in fats and oils and has been reported as a suitable biodegradable low molecular-weight additive for polyesters such as PHB, lowering its Tg continuously with an increase in the tributyrin content [16]. In previous works, we studied films based on blends of polylacticacid (PLA) and polyhydroxybutyrate (PHB) with tributyrin (TB) as plasticizer prepared by melt-compounding [7,17]. To the best of our knowledge, no other research works on PLA/PHB/TB systems have been previously reported. We analyzed the influence of PLA/PHB mass ratio and plasticizer content on thermal, uniaxial tensile and barrier properties of films. PLA/PHB blends containing different weight ratios (100/0, 70/30, 60/40, 50/50, 40/60, 30/70, 0/100) for a fixed plasticizer content (20 wt% TB) were first studied. We found that PLA-rich films, *i.e.* TB modified PLA/PHB 70/30 and 60/40, exhibited significantly improved tensile properties and ductility compared to pure PLA or PHB, and even to TB modified PLA and PHB. It is noticeable that TB was more effective than other plasticizers to enhance ductility of PLA/PHB blends, *i.e.* TB modified PLA/PHB 70/30 and 60/40 blends presented $\varepsilon_b \sim$ 190% and ~150%, respectively. We also investigated the effect of varying plasticizer content in PLA-rich films formulations. We determined that the incorporation of 15 wt% TB leads to films with the best balance between elongation capability and water permeation properties. In particular, PLA/PHB (70/30) film modified with 15 wt% TB showed not only relatively high elastic modulus, maximum stress and elongation at break, but also an average water vapor permeation (WVP) value which is similar to PLA."

When considering the performance of bio-based materials, the mechanical properties of most interest in packaging applications are without a doubt tensile strength and elongation, fracture toughness and impact strength. Much is published about tensile properties but fracture and impact characterization are often disregarded [18]. Keeping in mind that results of our previously developed materials are promising for a potential use as packaging materials, an exhaustive study of their mechanical behavior under severe loading conditions is still needed. Fracture toughness is indicative of the material's resistance to fracture in presence of a sharp crack. It is a very important feature since the existence of flaws is not completely avoidable in the processing of a material and is very common in polymeric films (e.g. different stress fields and material inhomogeneities, microvoids, density or orientation fluctuations in the polymer chain) [19]. On the other hand, impact strength is a measure of the materials' resistance to break when subjected to a sudden impact, such as falling during the transportation [18].

This research is mainly focused on the fracture behavior characterization of TB_PLA/PHB films, which according to our previous studies have shown the best balance between uniaxial tensile mechanical parameters and water permeation properties: 70/30 and 60/40 PLA/PHB blends modified with 15 wt% TB. For comparison purposes, samples of pristine and TB modified PLA and PHB are also included. The materials' fracture behaviors under two severe conditions - similar to those in service - are deeply studied: quasi-static loading and impact biaxial loading. Fracture toughness and impact resistance parameters are determined. Complementary evaluation on thermal, uniaxial tensile and water permeation properties is included in the discussion together with fracture characterization in order to understand TB_PLA/PHB materials properties relationships and films' performance. Finally, the capability of these materials as eco-friendly packaging films alternative is evaluated by comparing fracture toughness, uniaxial tensile and water permeation properties with those of commodities and other bio-based polymer systems used in this application.

2. Experimental

2.1. Materials and sample preparation

Poly(lactic acid) (PLA 2003D, Mw = 151 kg mol^{-1}, NatureWorks, USA) and poly(3-hydroxybutyrate) (PHB, Mw = 292 kg mol^{-1}, PHB Industrial S.A, Brazil), both supplied in pellets, were used to prepare polymer blends. Tributyrin (TB, Mw = 0.302 kg mol^{-1}, Fluka) was added as plasticizer.

Films' processing has been previously described in detail [17]. Briefly, PLA and PHB pellets were melt-mixed in different proportions in a double screw Haake mixer at 185 °C at 50 rpm during 3 min. PLA pellets were previously dried at 60 °C in a vacuum oven overnight. When added, TB content was fixed at 15 wt% PLA/PHB mass.

Blends were compression molded to obtain ~100 μm films in an EMS AMS 160/335DE hydraulic press. The processing temperature was 190 °C and the pressure was kept 1 min at 0.1 MPa and 2 min at 5 MPa. Finally, films were quenched at room temperature. Different film formulations were prepared: neat PLA, neat PHB, TB-modified PLA, TB-modified PHB, unmodified PLA/PHB blends and TB-modified PLA/PHB blends. Films samples' designations are given in Table 1 together with blends' formulation specification.

Double-edge notched-tension (DENT) and disk specimens for mechanical tests were cut from compression molded films. Samples' dimensions are shown in Fig. 1. In DENT specimens, double notches were introduced with a sharp razor blade (13 μm in diameter) in a device constructed on purpose that allowed their perfect alignment.

2.2. Fracture characterization at quasi-static loading conditions

Exploratory fracture tests were carried out on DENT samples in an INSTRON 4467 universal testing machine at room temperature (19 ± 1 °C) at a crosshead displacement rate of 1 mm min^{-1}. The notch length to sample width ratio was $a/W = 0.5$ as shown in Fig. 1. Different fracture methodologies were applied to evaluate fracture toughness of films depending on the fracture behavior displayed by DENT specimens. Fracture behavior was identified by the fracture surface appearance and the load-displacement curve shape along with the concept of ductility level (*D*) introduced by Martinez et al. [20]. For DENT specimens, *D* is defined as the ratio of displacement at rupture and initial ligament length (*L*). According to *D* value, fracture behavior is classified as brittle fracture ($D < 0.1$), ductile instability ($0.1 < D < 0.15$), post yielding ($0.15 < D < 1$), blunting ($1 < D < 1.5$) and necking ($D < 1.5$). In our films, brittle and post yielding fracture behavior regimens were identified.

2.2.1. Brittle behavior

For films that exhibited linear elastic response and brittle fracture, toughness was evaluated by means of the critical stress intensity factor at fracture initiation, K_{IQ}, according to Linear Elastic Fracture Mechanics (LEFM) [21]:

$$K_{Iq} = \frac{P_q}{B\sqrt{\frac{W}{2}}} f\left(\frac{a}{W}\right) \tag{1}$$
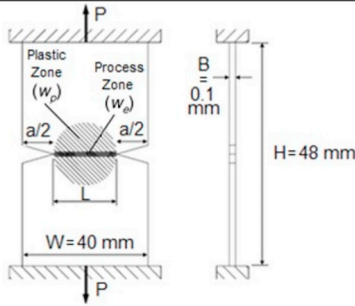
where P_q is the maximum peak load, B and W are the sample thickness and width, a is the notch length and $f(a/W)$ is given by:

$$f\left(\frac{a}{W}\right) = \frac{\sqrt{\frac{\pi a}{2W}}}{1 - \frac{a}{W}} \left[1.122 - 0.561\left(\frac{a}{W}\right) - 0.205\left(\frac{a}{W}\right)^2 + 0.471\left(\frac{a}{W}\right)^3 + 0.19\left(\frac{a}{W}\right)^4 \right] \tag{2}$$

Table 1
Film sample designation of TB_PLA/PHB films.

Material	Formulation (wt%)		
	PLA	PHB	TB
PLA	100	–	–
TB_PLA	85	–	15
PHB	–	100	–
TB_PHB	–	85	15
PLA/PHB:70/30	70	30	–
TB_PLA/PHB:70/30	59.5	25.5	15
TB_PLA/PHB:60/40	51	34	15

(a)

Fracture behavior	Fracture Parameter	Specimen dimension	Notch type	Test rate
Brittle	K_{IC}		Sharp $a/W = 0.5$	1 mm min⁻¹
Semi-brittle	J_c			
	K_c^E			
Ductile	w_e		Sharp $3B < L < W/3$	10 mm min⁻¹

(b)
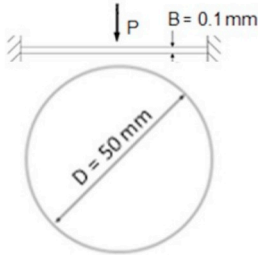
Test Configuration	Specimen dimension	Notch type	Test rate
Dart Impact		None	0.5 m s⁻¹

Fig. 1. Specimens' dimensions and fracture methodologies used in quasi-static DENT experiments (a) and dart impact experiments (b).

for DENT specimens [22]. At least five specimens with $a/W = 0.5$ were tested for each film composition.

2.2.2. Semi-brittle behavior

For films that displayed little plastic yielding at the crack tip before failure, fracture toughness was calculated following two methodologies: Equivalent Energy method [23] and J- Integral approach [24,25].

The equivalent stress intensity factor, K_c^E, was evaluated by replacing P_q in Eq. (1) by a pseudo-elastic load P^* [23]. P^* represents the maximum load achieved by a linear elastic material that displays the same deformation energy (U) than the specimen and it was obtained by extending the linear portion of the load-displacement curve up to reach U [26]. U was calculated integrating the actual load-displacement curve up to the fracture point.

The J-Integral at initiation, J_C, was evaluated at the instability load point as [27]:

$$J_C = \frac{\eta U}{B(W - a)} \qquad (3)$$

where U is the fracture energy (total area under the load-displacement curve), B, W and a are specimens dimensions and η is a geometry factor that for DENT specimens is expressed by Ref. [27]:

$$\eta = -0.06 + 5.99\left(\frac{a}{W}\right) - 7.42\left(\frac{a}{W}\right)^2 + 3.29\left(\frac{a}{W}\right)^3 \qquad (4)$$

At least five specimens with $a/W = 0.5$ were tested at 1 mm min⁻¹ for each film composition.

2.2.3. Post yielding behavior

For films that exhibited post yielding fracture behavior, fracture toughness was evaluated by means of the specific essential work of fracture, w_e, according to the Essential Work of Fracture (EWF) method [20,28–32]. This method is based on the partition of the total work of fracture (W_f) consumed during the fracture of a pre-cracked specimen, into the essential work required to fracture the polymer in its process zone and the non-essential or plastic work consumed by various deformation mechanisms in the plastic zone, as:

$$w_f = \frac{W_f}{LB} = w_e + \beta w_p L \qquad (5)$$

where w_f is the specific work of fracture (per unit ligament area), w_e is the specific essential work of fracture, w_p is the specific non-essential work of fracture (per unit volume), L and B are specimens' dimensions (Fig. 1-a) and β is a plastic zone shape factor. According to Eq. (5), w_e is determined as the intercept of the linear correlation of w_f versus L while βw_p is obtained from the slope. However, the following requirements must be meet to determine fracture toughness by EWF method: full ligament yielding before crack initiation, self-similarity in load–displacement curves to assure a common geometry of fracture and prevailing of plane-stress condition [32].

Clutton [28] proposed a criterion on the maximum stress values ($\sigma_{max} = P_{max}/L.B$) for DENT specimens by which it is possible to identify when the transition from plane-stress to a mixed stress state occurs. According to this protocol, the average value of maximum stress in ligament at yield, denoted as σ_m, is calculated and then maximum stress values might be greater than $0.9\sigma_m$ or less than $1.1\sigma_m$ so that the plane-stress condition prevails. The essential work data lying outside these limits should be eliminate.

At least 20 specimens of each film formulation were tested at 10 mm min⁻¹ and specimens' notches were within $3B \leq L \leq W/3$ ligament range. L was accurately measured with the aid of a PRAZIS PO-360-VD profile projector.

2.3. Fracture characterization at impact biaxial loading conditions

Dart impact experiments were then carried out on a Fractovis Ceast

6787 falling weight equipment at room temperature (19 ± 1 °C) at 0.5 m s^{-1}, using an instrumented high-speed dart with hemispherical 12.7 mm end onto disk specimens.

The thickness related energy (U/B) was calculated as the total energy to break the sample (being U the total area under the load-displacement curve) divided the thickness, B. Disk maximum strength (σ_d) was determined following [33]:

$$\sigma_d = 2.5 \frac{P_{max}}{B^2} \qquad (6)$$

2.4. Fracture surface morphology

In order to complete fracture characterization of films, the surface morphology of fractured DENT specimens was studied using a Field Emission Scanning Electron Microscope (FESEM Supra 25-Zeiss). Previously, samples were gold-sputtered to FESEM inspection. As shown in Fig. 2, two regions were examined, the fracture surface (region (a) in Fig. 2) and the plastic zone developed parallel to the load line direction (region (b) in Fig. 2).

2.5. Complementary characterization tests

In order to deeply understand TB_PLA/PHB behavior, we completed the thermal, tensile and barrier properties characterization carried out in previous works [7,17].

Materials were analyzed by scanning differential calorimetry (DSC) on a Pyris 1, PerkinElmer under nitrogen atmosphere at a flow rate of 20 mL/min. The temperature interval of measurements was from -50 to 190 °C at 10 °C/min, followed by a fast cooling until reaching -50 °C and a subsequent heating from -50 to 190 °C at 10 °C/min. Experiments were performed by triplicate. The average glass transition temperature (Tg) and melting temperature (Tm) were determined from the DSC curves and the degree of crystallinity (Xc) was calculated using the mass fraction of PLA in blends, the enthalpies of melting and cold crystallization of PLA and the theoretical melting enthalpy of PLA 100% crystalline (93 J/g) [8].

Tensile tests were performed following ASTM D1708-93 in a controlled atmosphere of 19 ± 1 °C using a universal testing machine, Instron 4467. Five specimens were tested for each blend formulation. The loading speed was 1 mm min^{-1} and the specimens presented a dumbbell shape. Average elastic modulus (E), yield stress (σ_y) and elongation at break (ϵ_b) were determined.

Barrier properties were characterized by means of the water vapor permeation (WVP) of materials, according to ASTM E 96-9500e1. Experiments were carried out by triplicate. The experimental setting consists in Teflon capsules of 5 cm in diameter filled with CaCl$_2$ as desiccant powder and sealed with the investigated films. Temperature and relative humidity were settled and controlled during the whole experiment at 18 °C and 65% RH. The water mass uptake of the desiccant powder was
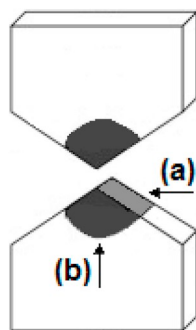
monitored over time until steady state is reached. WVP coefficients (g Pa^{-1} s^{-1} m^{-1}) of films were calculated using the water vapor transmission rate (WVTR), film thickness and partial vapor pressure gradient between both sides of the film.

3. Results and discussion

3.1. Fracture behavior at quasi-static loading conditions

Typical load-displacement curves obtained in exploratory fracture experiments are shown in Fig. 3. Raw load values are shown normalized by specimen's ligament area, $B(W-a)$, for comparison. Macroscopic pictures of some tested specimens are also included in Fig. 3 while fracture surfaces' morphologies are shown in Fig. 4.

Fracture behavior of TB_PLA/PHB DENT specimens markedly depends on film formulation. Three different fracture behaviors were identified: brittle, semi-brittle and ductile (post-yielding).

PHB films exhibit brittle behavior, as judged by the almost linear elastic P-d response (Fig. 3-a), the cracked feature of broken DENT specimens and the low D parameter value ($\sim$0.025). Fracture surface morphology shows typical signs of catastrophic failure through multiple crack planes (Fig. 4-a).

The incorporation of TB in PHB films causes a slight change in the fracture mode from brittle to semi-brittle. Crack propagation is unstable as it is evidenced by the abrupt drop in load-displacement curve (Fig. 3-a). However, TB_PHB specimens display larger D values than PHB specimens ($\sim$0.035). Normalized maximum load values achieved by TB_PHB specimens are quite lower than those of PHB specimens. Fracture occurs with little plastic yielding at the crack tip. Fracture surface morphology appears smoother than that of PHB specimen (Fig. 4-b).

PLA films display semi-brittle behavior with unstable crack propagation similar to TB_PHB films (Fig. 3-a). However, maximum normalized load and D parameter values ($\sim$0.054) are higher than TB_PHB ones.

The addition of TB in PLA films turns out the material to the ductile-to-brittle transition regime. In some specimens, failure occurs in a brittle manner while in others plastic yielding and stable crack propagation take place. This is evidenced in load-displacement curves and in tested specimens' features (Fig. 3-a). Fracture surface morphologies of specimens displaying both types of failure modes are completely different as well as their D values. Signs of material ductile tearing are detected in specimens that behave in a ductile manner (Fig. 4-d).

PLA/PHB:70/30 films also show semi-brittle fracture behavior. Maximum normalized load achieved by PLA/PHB:70/30 specimens practically coincides with that of PLA specimens as well as D parameter ($\sim$0.046). However, DENT specimen shows a stress-whitened region in the fracture process zone (Fig. 3-b). The inspection of fracture surface morphology revealed a PLA matrix with dispersed PHB particles (Fig. 4-e). The presence of voids indicates PHB particles debonding, which explains the macroscopic stress whitening observed in the specimen (Fig. 3-b).

The incorporation of TB in PLA/PHB:70/30 formulation caused a marked change in fracture propagation mode from unstable to stable and the overall fracture behavior from semi-brittle to ductile. D parameter value was large ($\sim$0.653) turning the material in the post-yielding fracture regime. This means that the material in the ligament area yielded before crack propagation initiation. A stress-whitened plastic zone with elliptical shape developed in TB_PLA/PHB:70/30 specimens parallel to the load line direction (Fig. 3-b). Fracture surface morphology shows extensive plastic deformation as it is evidenced by deformed large voids and PLA matrix ductile tearing (Fig. 4-f).

The change in PLA/PHB ratio from 70/30 to 60/40 in TB modified blends does not alter the ductile nature of fracture behavior. The features of tested specimens as well as fracture surface morphology result also very similar (Fig. 3-b and 4-g). However, TB_PLA/PHB:60/40 specimens display lower D parameters than TB_PLA/PHB:70/30

Fig. 2. Schematic of surfaces zones examined in FESEM experiments on postmortem DENT specimens: fracture surfaces (a) and plastic deformed zone (b).
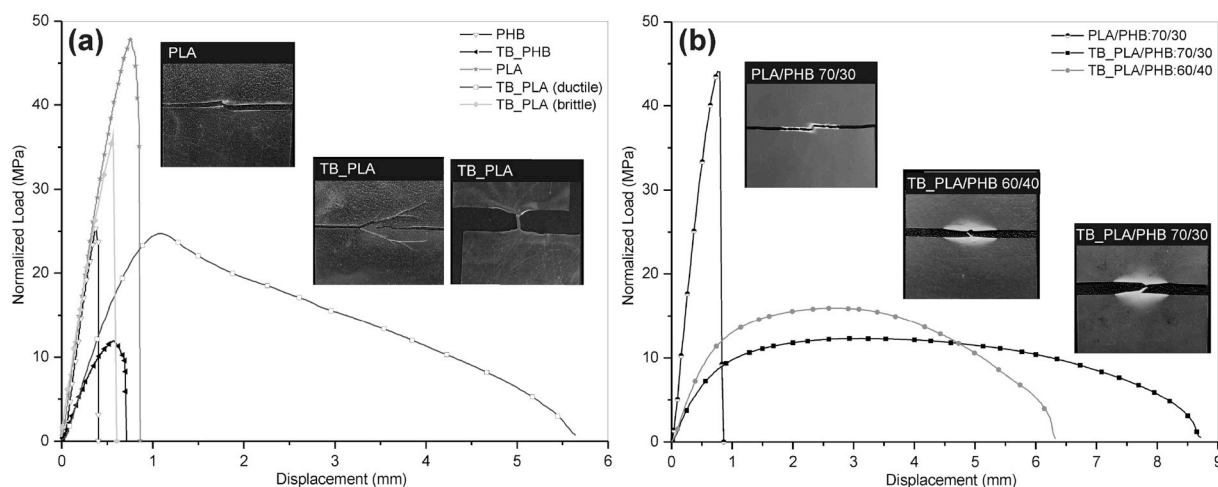
Fig. 3. Typical load-displacement curves obtained in exploratory fracture experiments of PLA, TB_PLA, PHB, TB_PHB (*a*); PLA/PHB:70/30 and TB_PLA/PHB blends (*b*); and images of post-mortem DENT specimens with $a/W = 0.5$ showing different fracture patterns (*inset*).
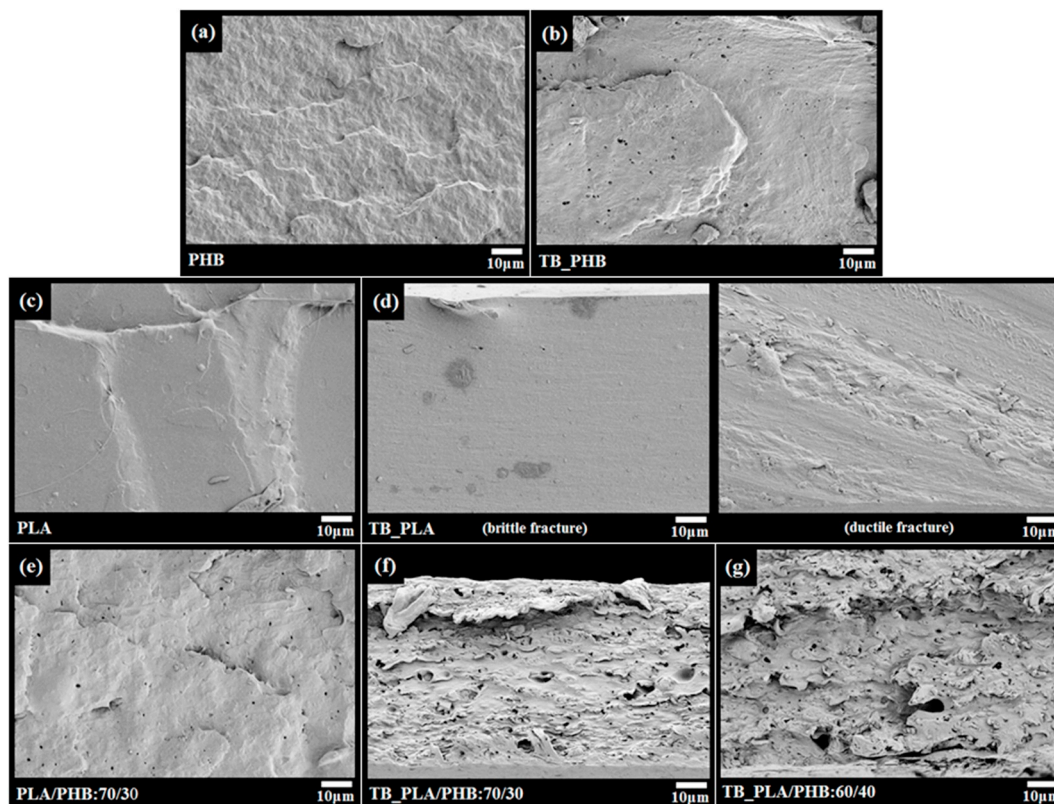

Fig. 4. FESEM micrographs of the fracture surfaces of post-mortem DENT specimens of PHB, TB_PHB, PLA, TB_PLA, PLA/PHB and TB_PLA/PHB blends.

(~0.418). Another noticeable difference is the morphology of the plastic zone region, as can be observed in Fig. 5. In TB_PLA/PHB:60/40 specimens a striated pattern apparently composed by subsurface multiple cracks is developed (Fig. 5-*b*). This may be related to differences in the phase morphology developed in the films for both formulations.

3.2. Fracture toughness determination at quasi-static loading conditions

3.2.1. Brittle and semi-brittle behavior

Fracture toughness parameter for the material that exhibit brittle fracture behavior (PHB) was evaluated by the LEFM K_{Iq} parameter. In this case, the J_c parameter based on the *J*-Integral approach is equal to

the LEFM G_c parameter [34]. For materials that exhibit semi-brittle behavior (TB_PHB, PLA, PLA/PHB:70/30), K_C^E and J_c were both evaluated. In the case of the material that behaved in the ductile to brittle transition regime (TB_PLA), only J_c was evaluated.

The determined parameters are shown in Table 2. Fracture toughness of PLA is higher than that of PHB and almost the same of PLA/PHB:70/30. The incorporation of TB does not improve fracture toughness of PHB films but turn out PLA into the ductile to brittle transition regime. This regime is characterized by a wide dispersion in fracture toughness values, as reflected in the standard deviation values reported in Table 2 for J_c data of TB_PLA sample.
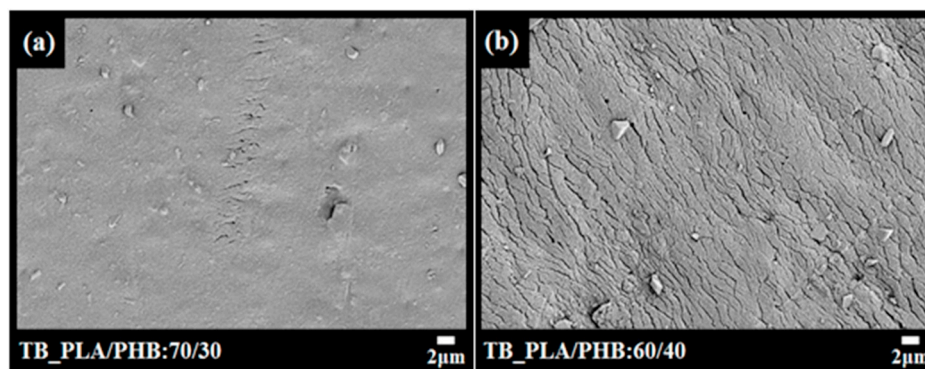
Fig. 5. FESEM images of the plastic zone developed parallel to the load line direction of TB_PLA/PHB blends.

Table 2
Fracture toughness parameters determined for PHB, TB_PHB, PLA, TB_PLA and PLA/PHB:70/30 films.

Material	K_{Iq} or K_c^E (MPa$\sqrt{m}$)	J_c (kJ/m^2)
PHB	3.7 ± 0.2	7.3 ± 0.4
TB_PHB	1.9 ± 0.4	5.2 ± 1.8
PLA	8.4 ± 0.6	33.2 ± 3.4
TB_PLA	–	29.8 ± 16.0
PLA/PHB:70/30	7.9 ± 1.6	28.0 ± 11.3

3.2.2. Post-yielding fracture behavior

Fracture behavior of TB-modified PLA/PHB blends was characterized by means of the Essential Work of Fracture (EWF) method. Typical load-displacement curves obtained for specimens with different ligament lengths are shown in Fig. 6.

The yielding of full ligament and stable crack propagation took place in all specimens and self-similarity of load–displacement curves is evidenced in Fig. 6. The Clutton's plane-stress criterion [28] was applied to all essential work data and the results of maximum stress (σ_{max}) as a function of ligament length (L) are shown in Fig. 7. It can be seen that for shorter ligaments σ_{max} rises, which reflects a change in stress state. These values have been eliminated from the EWF analysis. In addition, any data for which the maximum stress is higher than $1.1\sigma_m$ or lower than $0.9\sigma_m$, possibly arising from premature crack growth or simply experimental errors, have been excluded too. Then, the EWF procedure was applied to the remaining data.

Specific work of fracture (w_f) data for each material and for the

various ligament lengths were calculated by integrating the load-displacement curves and normalizing by the originals specimens' ligament area ($L.B$). Values were then plotted against ligament length (L) as shown in Fig. 8. Data were linearly fitted according to Eq. (5) using least squares method. Data lying outside the 95% confidence limits from the first best-fit line were eliminated from the analysis. Fracture parameters were obtained from a second linear fitting considering only valid data and listed in Table 3. The specific essential work of fracture parameter (w_e) represents the resistance to crack initiation and the slope of the w_f vs. L curve (βw_p) is related to the resistance to crack propagation. The former parameter depends on the initial structure of the material and the latter is strongly affected by the structural rearrangements induced by stress.

It can be seen that w_e values are similar for both blends (Table 3), i.e. the resistance to crack initiation seems to be affected by TB rather than PHB content. Regarding the βw_p parameter, it can be seen that the highest value corresponded to PLA/PHB: 70/30 (Table 3), which is consistent with the largest stress whitened zone developed in DENT samples (Fig. 3-b).

3.3. Fracture behavior at impact biaxial loading conditions

Biaxial impact tests give a realistic view of in service impact situations, being close to real life conditions. They provide a convenient method that is sensitive to changes induced by blends composition and morphology on final material performance [35].

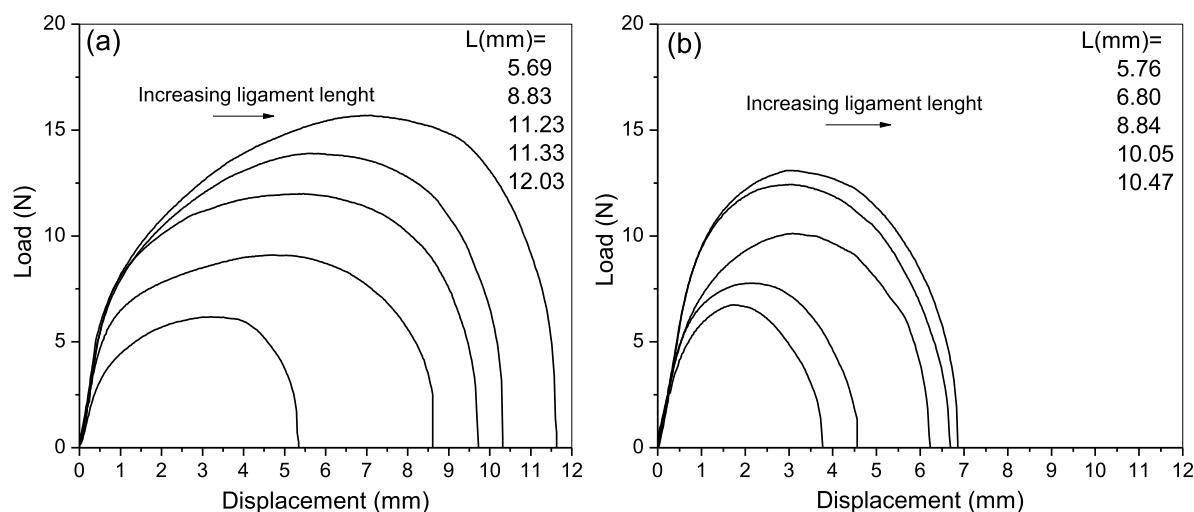Typical load displacement curves registered under impact loading

Fig. 6. Load-displacement curves for TB_PLA/PHB:70/30 (a) and TB_PLA/PHB:60/40 (b) films obtained for various ligament lengths.
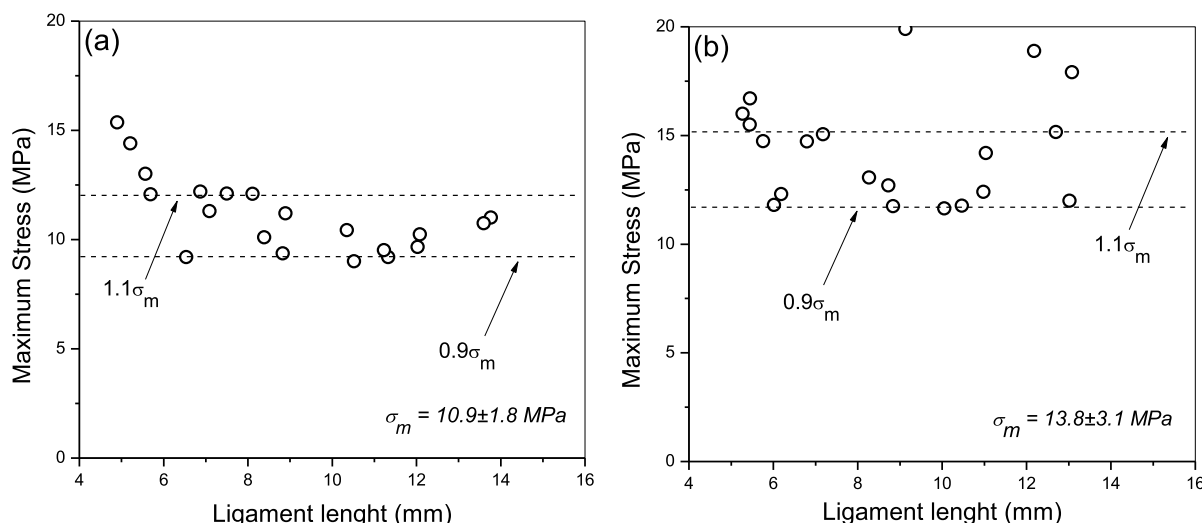
Fig. 7. Maximum stress in ligament at yield, σ_{max}, as a function of ligament length, L, for EWF experiments of TB_PLA/PHB:70/30 (a) and TB_PLA/PHB:60/40 films (b).
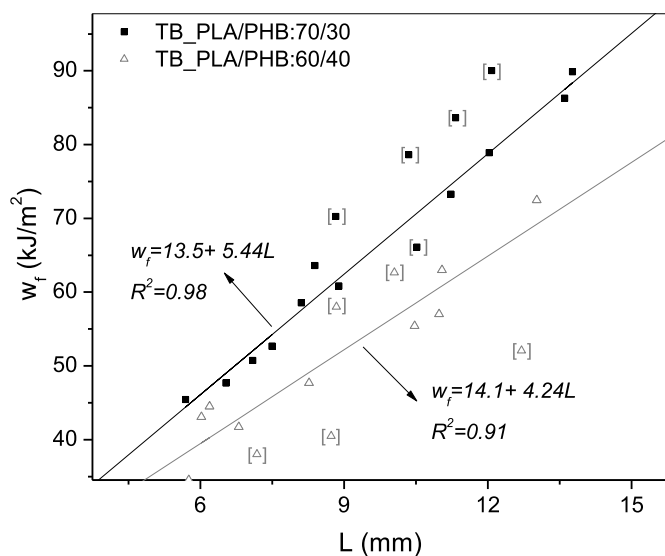

Fig. 8. Specific total work of fracture, w_f, versus ligament length, L, for TB_PLA/PHB samples.

Table 3
Fracture parameters of TB_PLA/PHB blends.

Material	w_e (kJ/m^2)	βw_p (MJ/m^3)
TB_PLA/PHB:70/30	13.5 ± 2.1	5.44 ± 0.22
TB_PLA/PHB:60/40	14.1 ± 4.2	4.24 ± 0.46

conditions are shown together with pictures of some broken samples in Fig. 9. Determined impact fracture parameters are listed in Table 4. Only a noise signal was registered when testing PHB samples due to the low load level required to break these samples (plot inserted in Fig. 9-*a*). For the other materials, all samples displayed a catastrophic failure showing an abrupt load drop at instability point. Most materials failed in a brittle mode, with the exception of TB_PLA/PHB samples. Ternary blends exhibited plastic deformation before failure as evidenced by non-linearity of load-displacement curves (Fig. 9-*b*), whitening of the impacted zone, and large energy absorption before failure (Table 4).

The addition of TB improves impact performance of both pristine polymers and blends: it increases both thickness related energy and maximum strength (Table 4). It is noticeable the case of TB_PLA, which displays a very large energy consumption before fracture. However, this large energy is only due to the formation of multiple cracks, with no plastic deformation.

3.4. Complementary characterization: TB_PLA/PHB blends' properties

The proposed TB_PLA/PHB systems are intended to be used as packaging materials. For this application, fracture behavior along with barrier, thermal and mechanical properties are crucial. In this section we summarize the complementary characterization results carried out in this and in own previous works properties [7,17].

Thermal properties determined from DSC tests are shown in Fig. 10. Blending PHB with PLA does not significantly affect thermal properties of PLA matrix. On the other hand, the incorporation of TB up to 20 wt% reduces Tg and Tm of PLA matrix and increases its crystalline degree. This is an expected effect that can be explained by the plasticizing effect of TB resulting in the increase of the molecular mobility of the polymer structure, then lowering glass transition temperatures [13]. The increase in chain mobility of PLA with TB shifts its melting temperature to lower values and enhances its ability to crystallize, increasing its crystallinity degree. On the other hand, it is evidenced that PHB acts as a nucleating agent for PLA crystallization [5,13]. Noticeably, the effect of TB and PHB in thermal properties of PLA matrix is accentuated in ternary blends. In TB_PLA/PHB materials containing 15 and 20 wt% TB, Tg of PLA matrix falls below room temperature, which markedly influences mechanical and fracture performance of these materials.

Uniaxial deformation properties obtained from tensile tests are shown in Fig. 11. As expected, the incorporation of TB decreases E and σ_y of pristine PLA and PHB polymers since it acts as a plasticizer. The reduction is more pronounced in TB_PLA/PHB blends with TB content larger than 10 wt%. The addition of TB over 10 wt% causes a large increase in ε_b of PLA/PHB blends, which is not observed in TB_PLA and TB_PHB materials. Therefore, if TB content is within 15 or 20 wt% range, a synergic effect in properties is obtained, leading to ternary blends with a striking enhancement in elongation capability with respect to pristine PLA, which is well correlated with the decrease in Tg.

Clearly, the change in mechanical properties of PLA with PHB and TB incorporation influences the fracture behavior under quasi-static and dynamic loading characterized in this work. The ductility parameter
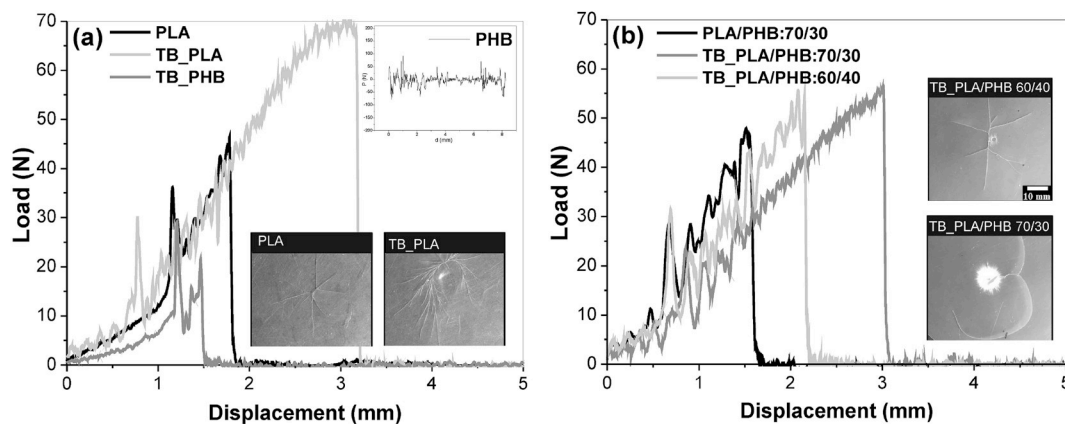
Fig. 9. Typical load-displacement curves of PLA, TB_PLA, TB_PHB and PHB in the inset (a); PLA/PHB:70/30 and TB_PLA/PHB blends (b); and images of tested specimens showing different fracture patterns under biaxial impact deformation (insets).

Table 4

Impact parameters of PLA, PHB and their blends (PLA/PHB and TB_PLA/PHB).

Material	U/B (J/m)	σ_d (GPa)
PLA	220 ± 27	7.2 ± 1.0
TB_PLA	1428 ± 411	16.1 ± 1.6
PHB	–	–
TB_PHB	90 ± 7	6.0 ± 0.3
PLA/PHB:70/30	159 ± 79	5.4 ± 1.3
TB_PLA/PHB:70/30	683 ± 48	7.4 ± 0.5
TB_PLA/PHB:60/40	424 ± 38	8.9 ± 0.8

obtained in quasi-static fracture mechanics of TB_PLA/PHB materials is shown in Fig. 12. The plasticizing effect of TB turns out the quasi-static fracture behavior of PHB from brittle to semi-brittle and of PLA from semi-brittle to the ductile to brittle transition regime, with a reduction in maximum stresses and increase in *D* parameters of DENT samples. A synergic effect is observed in PLA/PHB blends in which the addition of TB turns out the fracture behavior from semi-brittle to ductile. Fracture toughness values follow the trend observed in elastic modulus and yield stress (Fig. 11) in the case of materials with brittle and semi-brittle behaviors. The lower the yield stress and elastic modulus, the lower the fracture toughness is. In the case of TB_PLA/PHB blends, larger values of βw_p are in agreement with lower σ_y values [29,36]. Fracture performance under impact conditions is directly correlated with fracture behavior under quasi-static loading for studied materials. Therefore,
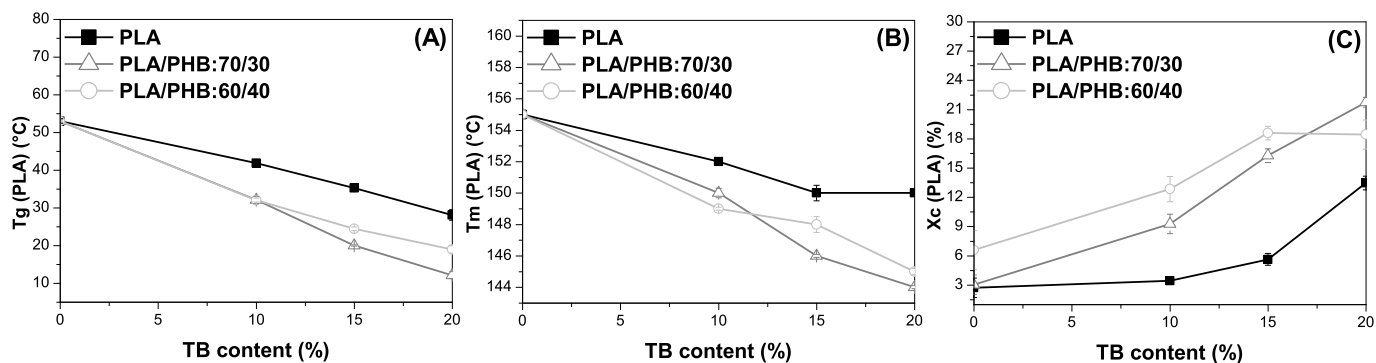

Fig. 10. Thermal properties of PLA based materials as a function of TB and PHB content: Glass transition temperature (*a*), melting temperature (*b*), degree of crystallinity (*c*).
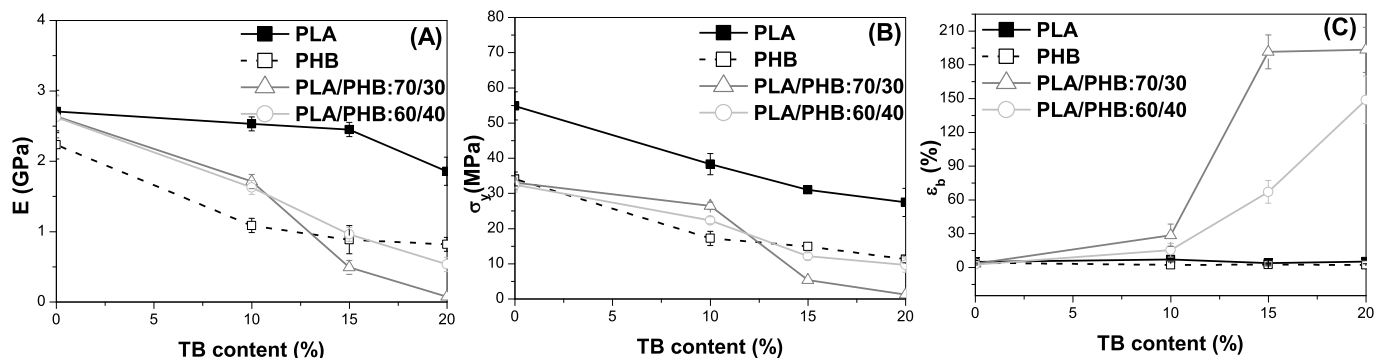

Fig. 11. Tensile properties of PLA based materials as a function of TB and PHB content: Elastic modulus (*a*), yield stress (*b*) and elongation at break (*c*).
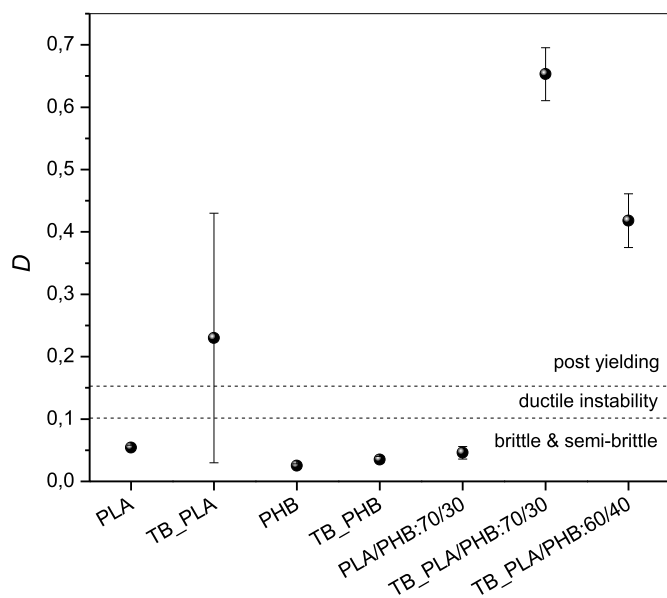
Fig. 12. Ductility level values of PLA, PHB, and PLA/PHB formulations.

TB_PLA/PHB blends exhibit higher ductility level than PLA under both severe fracture conditions.

Water permeation values of TB_PLA/PHB blends are shown in Fig. 13. Blending PHB with PLA improves barrier properties of pristine PLA. This positive effect in barrier properties may be due to the larger PLA crystallinity and the presence of the highly crystalline PHB [6]. However, the incorporation of TB increases WVP, or in other words, barrier properties are deteriorated. This detriment may be attributed to the larger free volume induced by the plasticizer addition, as previously observed in other PLA/PHB blends [6,13,37]. Therefore, TB induces two counteracting effects in water permeation efficiency: crystalline degree enhancement of PLA matrix and free volume increment in both PHB and PLA. Results demonstrate that the negative effect of free volume prevails for large TB content. WVP values of TB_PLA/PHB blends containing up to 15 wt% of TB reach the one of pristine PLA but with highly improved mechanical and fracture behaviors.
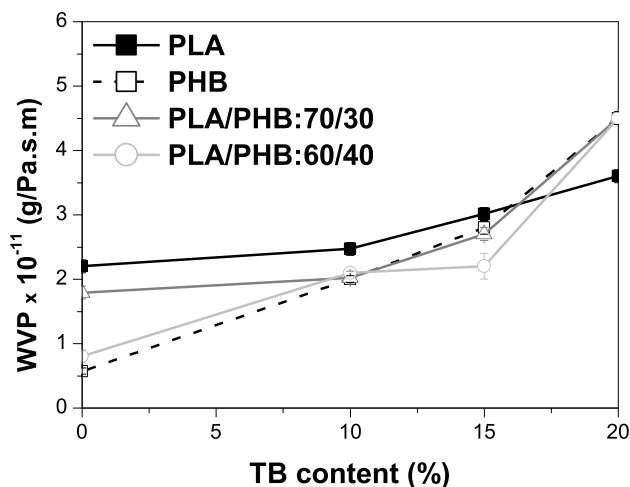

Fig. 13. Water vapor permeation (WVP) of PLA based materials as a function of TB and PHB content.

4. Evaluation of TB_PLA/PHB blends as suitable alternatives for packaging applications

The question to answer here is if permeation, tensile and fracture properties of TB_PLA/PHB films meet the requirements of packaging applications. We wonder whether TB_PLA/PHB blends are a suitable alternative to replace environment pollutant commodities overcoming drawbacks of currently used biodegradable polymers.

Polymers most frequently used by the packaging industry are polyethylene (PE), polypropylene (PP), polystyrene (PS), and polyethylene terephthalate (PET) [38]. High density PE is stiff, tough, easy to process and form, and resistant to moisture. It is used in applications such as bottles, box liners, and bags. Low-density PE is flexible, tough, relatively transparent, easy to seal, and resistant to moisture. It is mainly used in film applications like frozen food bags, flexible lids, and general-purpose containers. PP has good effectiveness as barrier to water vapor. It has a high melting point, making it ideal for hot-fill liquids and microwavable packaging. PS is generally foamed to produce an opaque, rigid and lightweight material with impact protection and thermal insulation properties. Typical applications include protective packaging, containers, disposable plastic silverware, lids, cups, plates, and trays. PET is glass-like transparent, lightweight, tough material, it has good gas and moisture barrier properties and good heat and chemical resistance. Hence, it is generally used to make containers, semi rigid sheets for thermoforming, and thin-oriented films [39]. However, PE, PP, PS and PET are derived from petroleum hydrocarbons, a nonrenewable source. In addition, they exhibit a very low biodegradation rate (150–1000 years), and therefore, waste accumulates polluting the environment.

Nowadays, also biodegradable polymers are being used for packaging. Besides PLA, most frequently used biopolymers are wheat gluten, cellophane and thermoplastic starches (TPS). Wheat gluten is generally use for edible films and coatings for foods. However, concerns remain regarding its high water adsorption and gas permeability [40]. Cellophane has good mechanical properties, hydrophilicity and low permeability to air, oils, greases, bacteria and water. It is tailor in thin and transparent sheets and generally used for food packaging [41]. TPS dominate the market of biogenerated polymers due to its environmental compatibility, wide availability, and low cost. Due to TPS moisture sensitivity and brittleness, it is generally used dispersed in poly(butylene adipate-*co*-terephthalate) (PBAT) and polycaprolactone (PCL) [42]. TPS/PBAT and TPS/PCL blends are used to package fresh and dry food, carrier bags, plates, glasses, and cutlery.

In Table 5, uniaxial tensile parameters, fracture toughness and water permeation property of TB_PLA/PHB blends are compared with those of the above mentioned petrochemical-based polymeric packaging materials and some biopolymers currently used for the intended application to answer our query. TB_PLA/PHB blends are not only fully bio-based and bio-compostable materials, but also exhibit better barrier properties and tensile performance than the other bio-materials included in the analysis.

TB_PLA/PHB blends show water vapor permeation, uniaxial tensile parameters and fracture toughness values within the range of those exhibited by PE materials even if the processing technique was not optimized and carried out at industrial scale. Regarding the comparison with commercial biodegradable and partly bio-based blends, TB_PLA/PHB blends exhibit improved fracture behavior with the additional advantage of being entirely obtained from renewable resources.

Although this comparison is far from being exhaustive, it is meaningful to highlight that proposed TB_PLA/PHB blends becomes a potential alternative for packaging application as flexible and tough films, broadening biodegradable PLA based polymers applications.

5. Conclusions

In this work, novel biobased TB_PLA/PHB materials are proposed as potential materials for replacement of commodities currently used in

Table 5
Properties of some traditional non-biodegradable petrochemical-based polymers and biodegradable bio-based and petro-based polymers used as packaging materials (the developed TB_PLA/PHB blends are included for comparison), from Refs. [19,32,41,43–61].

Property	Packaging materials											
	Biocompostable								Non–biocompostable			
	Bio-based						Partly bio-based	Petro-based	Petro-based			
	TB_PLA/PHB:70/30	TB_PLA/PHB:60/40	Wheat gluten	Cellophane	PLA	TPS	TPS/PBAT	PCL	PE	PP	PS	PET
Tensile modulus (GPa)	0.5	1	0.04	5.5	2–3	2.6	0.2	0.3	0.1–1	0.9–1.2	2.7–3.4	2.8–3.5
Tensile strength (MPa)	16	12	2.7	117	53	27	15	36	4–31	27–98	31–49	157–177
Tensile elongation at break (%)	191	67	197	3–14	2–6	1	376	430–850	20–800	120–1000	2–3	70–130
Fracture toughness (kJ/m^2)	13.5	14			6.5	3–11	0.001	30	11–27	6–14	1.1	35
WVP x 10^{11} (g Pa^{-1} s^{-1} m^{-1})	2.7	2.2	430	7.7–8.4	2–3	8.9	2	4	0.01–3	0.002–1.2	0.01–0.05	0.01–0.02

packaging applications. Fracture behavior of TB_PLA/PHB films is characterized under two severe loading solicitations, resembling in service conditions. In addition, thermal, tensile, water permeation and fracture properties are analyzed and compared to those of commodities and other biobased polymers.

Blending PLA with PHB enhances water permeation properties and crystalline degree of pristine PLA but mechanical and fracture properties are not improved. TB addition up to 15 wt% keeps water permeation near to those of pristine PLA. It also shifts PLA matrix Tg below room temperature, turning out quasi-static fracture behavior of PLA/PHB blends from semi-brittle to ductile and biaxial impact response from brittle to semi-ductile.

Uniaxial tensile parameters, fracture toughness and water permeation properties of TB_PLA/PHB films resulted to be close to those of polyethylene films used in packaging applications. Moreover, among currently used biobased materials, TB_PLA/PHB films show the best water permeation performance, almost the larger elongation capability and the highest fracture toughness.

Current work is in progress in order to optimize TB_PLA/PHB processing conditions, which we expected that further enhances films performance for packaging applications.

Declaration of competing interest

The authors declare that they have no known competing financial interests or personal relationships that could have appeared to influence the work reported in this paper.

CRediT authorship contribution statement

M.L. Iglesias Montes: Data curation, Investigation, Writing - original draft, Writing - review & editing. **V.P. Cyras:** Conceptualization, Funding acquisition, Writing - original draft, Writing - review & editing. **L.B. Manfredi:** Conceptualization, Funding acquisition, Writing - original draft, Writing - review & editing. **V. Pettarín:** Conceptualization, Investigation, Writing - original draft. **L.A. Fasce:** Conceptualization, Investigation, Visualization, Writing - original draft, Writing - review & editing.

Acknowledgements

Appendix A. Supplementary data

Supplementary data to this article can be found online at https://doi.org/10.1016/j.polymertesting.2020.106375.

Data availability

Processed data of the experimental results that validate the presented research findings are shown in the presented Figures and Tables. Additional data will be available on request.

References

[1] A.S. Luyt, Editorial corner – a personal view. Are we closer to a solution for the plastics waste disaster which faces the earth? Express Polym. Lett. 13 (2019) 937, https://doi.org/10.3144/expresspolymlett.2019.81.

[2] M. Jamshidian, E.A. Tehrany, M. Imran, M. Jacquot, S. Desobry, Poly-lactic acid: production, applications, nanocomposites, and release studies, Compr. Rev. Food Sci. Food Saf. 9 (2010) 552–571, https://doi.org/10.1111/j.1541-4337.2010.00126.x.

[3] H. Urayama, T. Kanamori, K. Fukushima, Y. Kimura, Controlled crystal nucleation in the melt-crystallization of poly(L-lactide) and poly(L-lactide)/poly(D-lactide) stereocomplex, Polymer 44 (2003) 5635–5641, https://doi.org/10.1016/S0032-3861(03)00583-4.

[4] A.J. Anderson, E.A. Dawes, Occurrence, metabolism, metabolic role, and industrial uses of bacterial polyhydroxyalkanoates, Microbiol. Rev. 54 (1990) 450–472.

[5] M. Zhang, N.L. Thomas, Blending polylactic acid with polyhydroxybutyrate: the effect on thermal, mechanical, and biodegradation properties, Adv. Polym. Technol. 30 (2011) 67–79, https://doi.org/10.1002/adv.20235.

[6] M.P. Arrieta, M.D. Samper, J. López, A. Jiménez, Combined effect of poly(hydroxybutyrate) and plasticizers on polylactic acid properties for film intended for food packaging, J. Polym. Environ. 22 (2014) 460–470, https://doi.org/10.1007/s10924-014-0654-y.

[7] M.L. Iglesias Montes, D.A. D'Amico, L.B. Manfredi, V.P. Cyras, Effect of natural glyceryl tributyrate as plasticizer and compatibilizer on the performance of bio-based polylactic acid/poly(3-hydroxybutyrate) blends, J. Polym. Environ. 27 (2019) 1429–1438, https://doi.org/10.1007/s10924-019-01425-y.

[8] M.A. Abdelwahab, A. Flynn, B.-S. Chiou, S. Imam, W. Orts, E. Chiellini, Thermal, mechanical and morphological characterization of plasticized PLA-PHB blends, Polym. Degrad. Stabil. 97 (2012) 1822–1828, https://doi.org/10.1016/j.polymdegradstab.2012.05.036.

[9] I. Armentano, E. Fortunati, N. Burgos, F. Dominici, F. Luzi, S. Fiori, A. Jiménez, K. Yoon, J. Ahn, S. Kang, J.M. Kenny, Bio-based PLA_PHB plasticized blend films: processing and structural characterization, LWT - Food Sci. Technol. (Lebensmittel-Wissenschaft -Technol.) 64 (2015) 980–988, https://doi.org/10.1016/j.lwt.2015.06.032.

[10] V. Jost, R. Kopitzky, Blending of polyhydroxybutyrate-co-valerate with polylactic acid for packaging applications – reflections on miscibility and effects on the mechanical and barrier properties, Chem. Biochem. Eng. Q. 29 (2015) 221–246, https://doi.org/10.15255/CABEQ.2014.2257.

[11] M.P. Arrieta, J. López, A. Hernández, E. Rayón, Ternary PLA-PHB-Limonene blends intended for biodegradable food packaging applications, Eur. Polym. J. 50 (2014) 255–270, https://doi.org/10.1016/j.eurpolymj.2013.11.009.

[12] Y. Ma, Y. Wang, Development of PLA - PHB - Based Biodegradable Active Packaging and its Application to Salmon, 2018, pp. 1–8, https://doi.org/10.1002/pts.2408.

[13] I. Armentano, E. Fortunati, N. Burgos, F. Dominici, F. Luzi, S. Fiori, A. Jiménez, Processing and characterization of plasticized PLA/PHB blends for biodegradable multiphase systems 9 (2015) 583–596, https://doi.org/10.3144/expresspolymlett.2015.55.

[14] M.P. Arrieta, E. Fortunati, F. Dominici, J. López, J.M. Kenny, Bionanocomposite films based on plasticized PLA-PHB/cellulose nanocrystal blends, Carbohydr. Polym. 121 (2015) 265–275, https://doi.org/10.1016/j.carbpol.2014.12.056.

[15] S. Wang, P. Ma, R. Wang, S. Wang, Y. Zhang, Y. Zhang, Mechanical, thermal and degradation properties of poly(d,l-lactide)/poly(hydroxybutyrate-co-hydroxyvalerate)/poly(ethylene glycol) blend, Polym. Degrad. Stabil. 93 (2008) 1364–1369, https://doi.org/10.1016/j.polymdegradstab.2008.03.026.

[16] N. Yoshie, K. Nakasato, M. Fujiwara, K. Kasuya, H. Abe, Y. Doi, Y. Inoue, Effect of low molecular weight additives on enzymatic degradation of poly(3-hydroxybutyrate), Polymer 41 (2000) 3227–3234, https://doi.org/10.1016/S0032-3861(99)00547-9.

[17] D.A. D'Amico, M.L. Iglesias Montes, L.B. Manfredi, V.P. Cyras, Fully bio-based and biodegradable polylactic acid/poly(3-hydroxybutirate) blends: use of a common plasticizer as performance improvement strategy, Polym. Test. 49 (2016) 22–28, https://doi.org/10.1016/j.polymertesting.2015.11.004.

[18] A. Emblem, Packaging technology: fundamentals, materials and processes, in: Plastics Properties for Packaging Materials, first ed., Woodhead Publishing Limited, London, UK, 2012 https://doi.org/10.1533/9780857095701.2.287. Ch. 13.

[19] F. Tuba, L. Oláh, P. Nagy, Characterization of reactively compatibilized poly(d,l-lactide)/poly(ε-caprolactone) biodegradable blends by essential work of fracture method, Eng. Fract. Mech. 78 (2011) 3123–3133, https://doi.org/10.1016/j.engfracmech.2011.09.010.

[20] A.B. Martinez, J. Gamez-Perez, M. Sanchez-Soto, J.I. Velasco, O.O. Santana, M. Ll Maspoch, The essential work of fracture (EWF) method - analyzing the post-yielding fracture mechanics of polymers, Eng. Fail. Anal. 16 (2009) 2604–2617, https://doi.org/10.1016/j.engfailanal.2009.04.027.

[21] J.G. Williams, M.J. Cawood, European group on fracture: Kc and Gc methods for polymers, Polym. Test. 9 (1990) 15–26, https://doi.org/10.1016/0142-9418(90)90045-F.

[22] M.A. Costantino, V. Pettarin, A.J. Pontes, P.M. Frontini, Mechanical performance of double gated injected metallic looking polypropylene parts, Express Polym. Lett. 9 (2015) 1040–1051, https://doi.org/10.3144/expresspolymlett.2015.93.

[23] F.J. Witt, The equivalent energy method: an engineering approach to fracture, Eng. Fract. Mech. 14 (1981) 171–187, https://doi.org/10.1016/0013-7944(81)90026-6.

[24] E. Plati, J.G. Williams, The determination of the fracture parameters for polymers in impact, Polym. Eng. Sci. 15 (1975) 470–477, https://doi.org/10.1002/pen.760150611.

[25] ASTM E1820, Standard Test Method for Measurement of Fracture Toughness, 1996.

[26] ASTM E992-89, Practice for Determination of Fracture Toughness of Steels Using Equivalent Energy Methodology, 1997.

[27] L.A. Fasce, V. Costamagna, V. Pettarin, M. Strumia, P.M. Frontini, Poly(acrylic acid) surface grafted polypropylene films : near surface and bulk mechanical response 2 (2008) 779–790, https://doi.org/10.3144/expresspolymlett.2008.91.

[28] E.Q. Clutton, ESIS TC4 experience with the essential work of fracture method, Eur. Struct. Integr. Soc. 27 (2000) 187–199, https://doi.org/10.1016/S1566-1369(00)80018-7.

[29] J. Gámez-Pérez, J.C. Velazquez-Infante, E. Franco-Urquiza, P. Pages, F. Carrasco, O.O. Santana, M.L. Maspoch, Fracture behavior of quenched poly(lactic acid), Express Polym. Lett. 5 (2011) 82–91, https://doi.org/10.3144/expresspolymlett.2011.9.

[30] J. Karger-Kocsis, E.J. Moskala, Molecular dependence of the essential and non-essential work of fracture of amorphous films of poly (ethylene-2, 6-naphthalate) (PEN), Polymer 41 (2000) 6301–6310.

[31] D. Ferrer-Balas, M.L. Maspoch, Y.W. Mai, Fracture behaviour of polypropylene films at different temperatures: fractography and deformation mechanisms studied by SEM, Polymer 43 (2002) 3083–3091, https://doi.org/10.1016/S0032-3861(02)00102-7.

[32] T. Bárány, T. Czigánya, J. Karger-Kocsis, Application of the essential work of fracture (EWF) concept for polymers, related blends and composites: a review, Prog. Polym. Sci. 35 (2010) 1257–1287, https://doi.org/10.1016/j.progpolymsci.2010.07.001.

[33] D.P. Jones, D.C. Leach, D.R. Moore, The application of instrumented falling weight impact techniques to the study of toughness in thermoplastics, Deform. Yield Fract. Polym. VI (1985) 27.

[34] D.R. Moore, A. Pavan, J.G. Williams, Fracture mechanics testing methods for polymers, adhesives and composites, Eur. Struct. Integr. Soc. 28 (2001).

[35] C.B. Bucknall, D.R. Paul, Characterizing toughness using standard empirical tests, Polym. Blends 2 (2000) 25–27.

[36] A. Arkhireyeva, S. Hashemi, Fracture behaviour of polyethylene naphthalate (PEN), Polymer 43 (2002) 289–300, https://doi.org/10.1016/S0032-3861(01)00623-1.

[37] N. Burgos, V.P. Martino, A. Jiménez, Characterization and ageing study of poly (lactic acid) films plasticized with oligomeric lactic acid, Polym. Degrad. Stabil. 98 (2013) 651–658, https://doi.org/10.1016/j.polymdegradstab.2012.11.009.

[38] K. Marsh, B. Bugusu, Food packaging - roles, materials, and environmental issues: scientific status summary, J. Food Sci. 72 (2007), https://doi.org/10.1111/j.1750-3841.2007.00301.x.

[39] A. Arora, G.W. Padua, Review: nanocomposites in food packaging, J. Food Sci. 75 (2010) 43–49, https://doi.org/10.1111/j.1750-3841.2009.01456.x.

[40] P.S. Tanada-Palmu, C.R.F. Grosso, Development and characterization of edible films based on gluten from semi-hard and soft Brazilian wheat flours (development of films based on gluten from wheat flours), Ciência Tecnol. Aliment. 23 (2003) 264–269, https://doi.org/10.1590/s0101-20612003000200027.

[41] C. Shi, S. Zhang, M. Li, W. Sun, G. Fan, Y. Jin, J. Yang, T. Dong, Barrier and mechanical properties of biodegradable poly(ε- caprolactone)/cellophane multilayer film, J. Appl. Polym. Sci. 130 (2013) 1805–1811, https://doi.org/10.1002/app.39354.

[42] P. Ma, Tailoring the Properties of Bio-Based and Biocompostable Polymer Blends, Netherlands Ipskamp Druk. Print, Eindhoven, 2011, https://doi.org/10.6100/IR712662.

[43] M. Ghasemlou, N. Aliheidari, R. Fahmi, S. Shojaee-Aliabadi, B. Keshavarz, M. J. Cran, R. Khaksar, Physical, mechanical and barrier properties of corn starch films incorporated with plant essential oils, Carbohydr. Polym. 98 (2013) 1117–1126, https://doi.org/10.1016/j.carbpol.2013.07.026.

[44] M.U. Haque, A. Stocchi, V. Alvarez, M. Pracella, Fracture behaviour of biodegradable polymer/polyolefin-natural fibers ternary composites systems, Fibers Polym. 15 (2014) 2625–2632, https://doi.org/10.1007/s12221-014-2625-2.

[45] H. Liu, J. Zhang, Research progress in toughening modification of poly(lactic acid), J. Polym. Sci., Part B: Polym. Phys. 49 (2011) 1051–1083, https://doi.org/10.1002/polb.22283.

[46] M. Tanaka, S. Ishizaki, T. Suzuki, R. Takai, Water vapor permeability of edible films prepared from fish water soluble proteins as affected by lipid type, J. Tokyo Univ. Fish 87 (2001) 31–37. http://id.nii.ac.jp/1342/00000089/.

[47] F. Tihminlioglu, I.D. Atik, B. Özen, Water vapor and oxygen-barrier performance of corn-zein coated polypropylene films, J. Food Eng. 96 (2010) 342–347, https://doi.org/10.1016/j.jfoodeng.2009.08.018.

[48] F. Touchaleaume, L. Martin-Closas, H. Angellier-Coussy, A. Chevillard, G. Cesar, N. Gontard, E. Gastaldi, Performance and environmental impact of biodegradable polymers as agricultural mulching films, Chemosphere 144 (2016) 433–439, https://doi.org/10.1016/j.chemosphere.2015.09.006.

[49] Y. Wang, Y. Qin, Y. Zhang, M. Yuan, H. Li, M. Yuan, Effects of N-octyl lactate as plasticizer on the thermal and functional properties of extruded PLA-based films, Int. J. Biol. Macromol. 67 (2014) 58–63, https://doi.org/10.1016/j.ijbiomac.2014.02.048.

[50] F. Yahiaoui, F. Benhacine, H. Ferfera-Harrar, A. Habi, A.S. Hadj-Hamou, Y. Grohens, Development of antimicrobial PCL/nanoclay nanocomposite films with enhanced mechanical and water vapor barrier properties for packaging applications, Polym. Bull. 72 (2014) 235–254, https://doi.org/10.1007/s00289-014-1269-0.

[51] S.D. Park, M. Todo, K. Arakawa, Effect of annealing on fracture mechanism of biodegradable poly(lactic acid), Key Eng. Mater. (2004) 261–263, 105–110, https://doi.org/10.4028/www.scientific.net/KEM.261-263.105.

[52] I. Zembouai, M. Kaci, S. Bruzaud, A. Benhamida, Y.M. Corre, Y. Grohens, A study of morphological, thermal, rheological and barrier properties of Poly(3-hydroxybutyrate-Co-3-Hydroxyvalerate)/polylactide blends prepared by melt mixing, Polym. Test. 32 (2013) 842–851, https://doi.org/10.1016/j.polymtesting.2013.04.004.

[53] M. Zhang, Development Of Polyhydroxybutyrate Based Blends for Compostable Packaging, 2011. Dr. Diss. © Min Zhang.

[54] X. Zhang, M.D. Do, K. Dean, P. Hoobin, I.M. Burgar, Wheat-gluten-based natural polymer nanoparticle composites, Biomacromolecules 8 (2007) 345–353, https://doi.org/10.1021/bm060929x.

[55] L. Bastarrachea, S. Dhawan, S.S. Sablani, Engineering properties of polymeric-based antimicrobial films for food packaging, Food Eng. Rev. 3 (2011) 79–93, https://doi.org/10.1007/s12393-011-9034-8.

[56] M. Bertuzzi, M. Armada, J. Gottifredi, Estudio de la permeabilidad al vapor de agua de films comestibles para recubrir alimentos, 2002, pp. 1–10. Editorial.Unca.Edu. Ar.

[57] N. Burgos, I. Armentano, E. Fortunati, F. Dominici, F. Luzi, S. Fiori, F. Cristofaro, L. Visai, A. Jimenez, J.M. Kenny, Functional properties of plasticized bio-based poly(lactic Acid)_Poly(hydroxybutyrate) (PLA_PHB) films for active food packaging, Food Bioprocess Technol. 10 (2017) 770–780, https://doi.org/10.1007/s11947-016-1846-3.

[58] Y.P. Chang, A. Abd Karim, C.C. Seow, Interactive plasticizing-antiplasticizing effects of water and glycerol on the tensile properties of tapioca starch films, Food Hydrocolloids 20 (2006) 1–8, https://doi.org/10.1016/j.foodhyd.2005.02.004.

[59] P.A. Dilara, D. Briassoulis, Standard testing methods for mechanical properties and degradation of low density polyethylene (LDPE) films used as greenhouse covering materials: a critical evaluation, Polym. Test. 17 (1998) 549–585, https://doi.org/10.1016/S0142-9418(97)00074-3.

[60] M.A. Garcia, A. Pinotti, N.E. Zaritzky, Physicochemical, water vapor barrier and mechanical properties of corn starch and chitosan composite films, Starch Staerke 58 (2006) 453–463, https://doi.org/10.1002/star.200500484.

[61] A. Gennadios, A.H. Brandenburg, J.W. Park, C.L. Weller, R.F. Testin, Water vapor permeability of wheat gluten and soy protein isolate films, Ind. Crop. Prod. 2 (1994) 189–195, https://doi.org/10.1016/0926-6690(94)90035-3.